International Journal of Sustainable Intelligent Technologies
ISSN: 3139-1249
IJSIT-05

INVESTIGATING SPIN-ORBIT TORQUES IN A CO/PT BILAYER USING FIRST PRINCIPLES CALCULATIONS

Dr. VSR Kumari, *Professor in Dept of ECE & Principal*,
Sai Spurthy Institute of Technology(Autonomous), Sathupally

ABSTRACT:The spin-orbit torque in a disordered Co/Pt bilayer is estimated using a non-equilibrium Green's function formalism. The torque has two formal components: Fermi-surface and Fermi-sea contributions. The Fermi-surface component dominates at low temperatures, while the Fermi-sea term is substantial at normal temperatures. In addition to the typical field-like and damping effects, the odd torque has a considerable planar Hall-like component (m E)m (z m), which contributes to damping. While field-like torques on Pt atoms do not require spin-orbit coupling, it is primarily responsible for torques that contribute to damping.

Keywords:*Spin-orbit torque; Co/Pt bilayer; First-principles calculations; Density functional theory (DFT); Spin-orbit coupling; Spin Hall effect; Magnetization dynamics.*

1. INTRODUCTION

Spin-orbit torque (SOT), a physical embodiment of relativistic physics in the solid state, has sparked widespread interest due to potential applications in memory technologies and spin-torque nano-oscillators. SOT can exist in formations without bulk inversion symmetry or structural inversion symmetry, such as (Ga,Mn)As crystals. This phenomenon affects magnetization dynamics and is characterized by nonequilibrium spin density. For systems with a heavy metal/ferromagnet interface, two SOT mechanisms have been proposed: the bulk spin-Hall effect, which originates in the heavy metal, and the inverse spin-galvanic effect, which occurs at the heavy metal/ferromagnet contact. The terms produced by these mechanisms in SOT are odd in proportion to the magnetization denoted by the unit vector m, and even in relation to damping-like m × [(z × E) × m]. However, basic models fail to capture all of the components of SOT. Symmetry allows for additional terms with more intricate angular dependences, which have been empirically determined in a variety of systems. The bulk spin-Hall effect is not required for these contributions; they can be attributed purely to interfacial scattering. Furthermore, insufficient crystallographic symmetry has been discovered to cause axisally asymmetric contributions to SOT.

SOT bilayers typically have layer thicknesses of less than one nanometer. As a result, it is critical to offer a comprehensive quantum-mechanical description of the complete apparatus; both the phenomenological concept of a boundary between bulk areas and the interpretation based on the bulk spin-Hall effect are unjustified. The extreme situation of a magnetic layer in contact with a topological insulator (TI) produces a high SOT. Recent research indicates that bulk and interface contributions to damping-like SOT are in competition. Furthermore, ab initio studies with Pt/Py bilayers highlight the significance of interfacial contributions to the spin-Hall effect.

Previous studies into SOT ab initio fail to fully grasp its physics due to the use of

DOI : https://doi.org/10.5281/zenodo.22326694

phenomenological broadening for Green's functions. This letter describes the work made in developing the non-equilibrium Green's function (NEGF) method for ab initio computations of the muffin-tin orbital (SOT) in magnetic multilayered systems. The LMTO approach clearly accounts for disorder in the NEGF. Following that, we will apply this approach to explore SOT in a Co/Pt bilayer. SOT exhibits a complex angular dependence, with a significant planar Hall-like contribution, according to our findings.

Spin-orbit coupling is used in our LMTO-NEGF treatment to alter the second-order LMTO potential parameters. To calculate atom i's spin torque, use the atomic sphere integral (Ti) = R Bxc,in(r)×mout(r)d 3 ri. The symbol "Bxc,in(r)" indicates the "input" exchange-correlation field, which corresponds to the stated direction of magnetization, whereas "mot(r)" represents the "output" magnetization obtained from the NEGF computation. This technique is supported by the use of constraining fields, which stabilize the immediate orientation of magnetization and balance the internal spin torque with the constraining field torque. The matrix of spin density

$$\hat{\rho}(\mathbf{r}) = -\frac{i}{2\pi}\int_{-\infty}^{\infty} \hat{G}_{<}(E,\mathbf{r},\mathbf{r})dE$$

The Keldysh formalism's Green's function (G^) yields

$$G_{<} = iG\left(f_L\Gamma_L + f_R\Gamma_R\right)G^{\dagger},$$

The occupation function for the two leads is written as fL/R(E). The anti-Hermitian part of the selfenergy for lead L (left) or R (right) is denoted as ΔL/R. The delayed and advanced Green's functions are G and G–. When bias V is applied, the potential of the left (right) lead and the chemical potential shift symmetrically by ±eV/2. In steady state, a homogeneous metallic conductor with bias V has a linear potential drop between its leads.

The integral in Equation can be obtained by applying the identity G(vL + ξR)G– = i(G - G–). This integral consists of two formal components: the Fermi-surface and Fermi-sea contributions.

$$\hat{\rho}_{sea}(\mathbf{r}) = \frac{i}{2\pi}\int \bar{f}(E)(G - G^{\dagger})dE$$
$$\hat{\rho}_{F}(\mathbf{r}) = \frac{eV}{4\pi}\int \left(-\frac{\partial \bar{f}}{\partial E}\right) G(\Gamma_L - \Gamma_R)G^{\dagger}dE$$

The distinction between (4), which preserves only the linear term, and ·f, which reflects the Fermi function with the unchanged chemical potential, is not exclusive and serves as a practical gauge selection [54]. The bias enters the Fermi-sea contribution (3) via a linear potential reduction. The Fermi-sea term is a possible source of magnetization damping.

An inspection is performed on a bilayer made up of six Co and Pt monolayers. The atoms are placed on sites of the ideal face-centered cubic (fcc) lattice, which is almost halfway between the sites of fcc Co and Pt and has a lattice parameter of 3.75 A. The interface is now oriented in the direction of and measured along the (001) plane. Four monolayers of empty spheres are used to approximate vacuum conditions and separate the free surfaces. The active zone,

DOI : https://doi.org/10.5281/zenodo.22326694

International Journal of Sustainable Intelligent Technologies
ISSN: 3139-1249
IJSIT-05

which measures 120 m, is currently under review.

Figure 1 shows the bilayer's band structure near the Fermi level. Spin-orbit coupling combines the majority and minority spin states, resulting in many avoided crossings. Because of the complicated dispersion of bands crossing the Fermi level, first-principles calculations may be required for quantitative material-specific predictions.

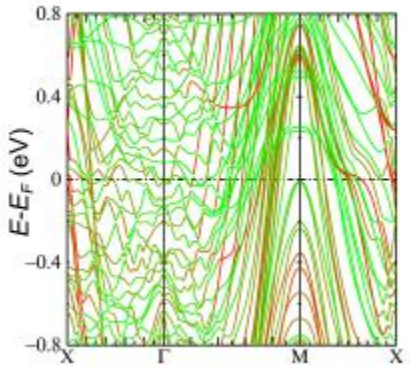

Figure 1 shows the spin-orbit interaction of the Co/Pt bilayer band structure. The hues red and green represent the majority and minority's spin properties, respectively.

Thin-film bilayers utilized in SOT investigations have high resistivities (20-100 μΩ•cm), indicating disorder. The principal defect types causing the high residual resistivity are unknown. To describe this disorder generally, we use the Anderson disorder model. Each site i, including empty spheres, is treated to a random potential Vi with a uniform distribution within the range −Vm< Vi <Vm. The following equation was used to illustrate the disorder model.

The equation T = Te+To, where m is an odd integer and To is an even number, cuts the total torque T in half. The bilayer has C4v crystallographic symmetry. The z-axis corresponds to the current orientation, and the x-axis corresponds to the film plane's normal. The allowed terms in the SOT angular dependency are established by group-theoretic analysis:

$$\mathbf{T}_e = P(\{A\},\theta)\,\mathbf{m}\times[(\mathbf{z}\times\mathbf{E})\times\mathbf{m}] + P(\{A'\},\theta)\,(\mathbf{m}\cdot\mathbf{E})\,\mathbf{z}\times\mathbf{m} + P(\{A_\alpha\},\theta)\,m_z\left(m_x^2-m_y^2\right)\mathbf{m}\times(E_x,-E_y,0) + P(\{A_\beta\},\theta)\left[\left(m_x^2-m_y^2\right)(\mathbf{m}\times\mathbf{z})(E_x m_x - E_y m_y) - \langle\ldots\rangle\right] + \cdots$$

$$\mathbf{T}_o = P(\{B\},\theta)\,(\mathbf{z}\times\mathbf{E})\times\mathbf{m} + P(\{B'\},\theta)\,(\mathbf{m}\cdot\mathbf{E})\,\mathbf{m}\times(\mathbf{z}\times\mathbf{m}) + P(\{B_\alpha\},\theta)\left(m_x^2-m_y^2\right)\mathbf{m}\times(E_y,E_x,0) + \cdots$$

X2n, where n = 0, 1, is a set of coefficients represented by {X}. The linear combination of even Legendre polynomials is: P({X}, θ) = P n X2nP2n(cos θ). In a system with axial symmetry group C∞v, the A, A0, B, and B0 terms are allowed. However, when the symmetry is reduced to C4v, the Aα, Aβ, and Bα terms appear. H brackets. As in Equation. indicate the previous term's average over the bilayer's axial rotations, proportional to the related A0 0 term. The averages for words Aα and Bα have already disappeared. The expected angular

DOI : https://doi.org/10.5281/zenodo.22326694

International Journal of Sustainable Intelligent Technologies
ISSN: 3139-1249
IJSIT-05

dependency in the axially symmetric polycrystalline sample with (001) texture may be calculated using only the A, A0, B, and B0 terms. The magnetoelectric coefficient [B/E] = ns/m = T • nm/V defines the torquances as τe = Te/(ME) and τo = To/(ME), where M represents the total magnetization. These values are utilized in all calculations with E = Exˆ. SOT influences the magnetization damping α determined from FMR line width measurements.

Δα is calculated as C(E/B).

$$C = \mathbf{m} \cdot \nabla_{\mathbf{m}} \times [\mathbf{m} \times \boldsymbol{\tau}(\mathbf{m})]$$

The negative curl of the effective field.

According to Eq., the Fermi-sea term is calculated in the device's middle using a symmetrically applied finite bias of order 1 mV. (3)-(4), in an ordered fashion. The equilibrium torque caused by magnetic anisotropy is eliminated by removing the torque at both positive and negative bias. In order to avoid the arduous task of evaluating the integral in Equ. (3), the Fermi-sea term at a finite temperature is calculated using the integration approach described in Ref. 55. Only a few spots on the imaginary axis necessitate the calculation of the integrand; most of these sites allow for a coarse mesh in the reciprocal-space integral. Following the computation of 61 magnetization orientations, the perfectly even Fermi sea term is fitted to Eq. (5). We demonstrated that the Fermi-sea torque is independent of the active region's length at constant field, is linearly dependent on the bias voltage, and vanishes when the linear potential drop at the active region's borders is substituted with two abrupt steps. Fig. displays the Fermi-sea torquances determined for T = 50, 100, 200, and 300 K. 2. The simplest set of terms that provide an acceptable fit at all temperatures are A0, A2, A0 0, and Aβ0 (refer to Table I). The parameter C is illustrated in Figure. is calculated using a more accurate multi-parametric fit. 2. At low temperatures, the maximum term in the minimal fit, A0 0, increases dramatically. At lower temperatures, A2 and Aβ0 are substantial, despite the fact that in polycrystalline samples, Aβ0 should be average.

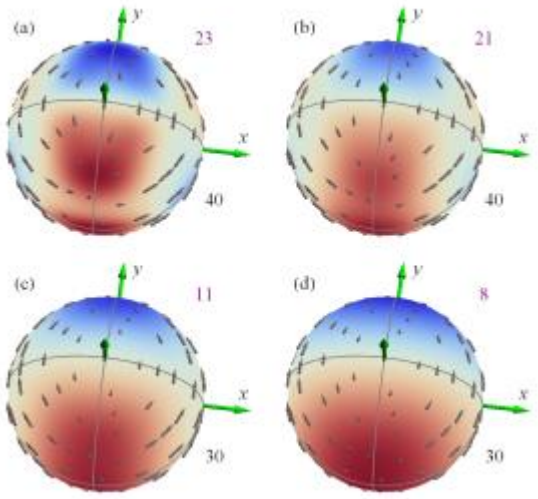

Fig. 2. Fermi sea contribution torque values for τe (arrows) at 50, 100, 200, and 300 K. The

DOI : https://doi.org/10.5281/zenodo.22326694

International Journal of Sustainable Intelligent Technologies
ISSN: 3139-1249
IJSIT-05

red (blue) color intensity represents the positive (negative) magnitude of the damping parameter C (Eq.). The number in the upper right corner of each panel indicates the color map scale, which is in nanometers per meter. The number in the lower right corner also indicates the scale of an arrow with a length equal to the sphere's radius.

Given the integrand in Eq. Only at the Fermi level EF is equation (4) for the Fermi-surface term need to be determined because it comprises a delta-function at zero temperature. To keep relative errors to a few percent, around 1000 points are required for reciprocal-space integration. The Fermi surface contribution to the overall torquance is computed and averaged over a sufficient number of disorder configurations for each of the 32 magnetization orientations, which result in 16 antiparallel lel pairs. Next, the symmetric and antisymmetric torque components are fitted to the equations. (5) As well as (6). Table I shows the only significant coefficients: A0, A0 2, B0, and B0 0. Except for A0 0, all coefficients show a slight reliance on the transverse supercell size Ly, demonstrating that disorder averaging is valid. Figure shows the results of evaluating the damping parameter C using the fitted formulas. 3 represents two disorder strengths (Vm = 0.77 and 1.54 eV).

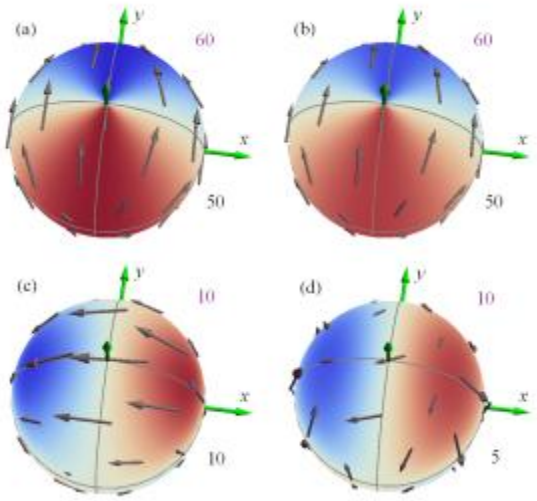

Figure 3 shows the Fermi surface contributions to torquance: (a) τe at Vm = 0.77 eV; (b) τe at Vm = 1.54 eV; (c) τo at Vm = 0.77 eV; and (d) τo at Vm = 1.54 eV. The scales for these contributions are shown in Figure 2. To average the diseases, we used supercells with Ly = 2.

A0, which is analogous to damping, dominates the Fermi-surface contribution to even torquance. C = −(2A0 + A0 0)my is the main contributor to damping from even torquance. Table I shows that, while the resistivity and resistance of the active region increase by more than a factor of two, the coefficient A0 essentially remains constant when the disorder strength grows from 0.77 to 1.54 eV. This shows that the damping-like torque A0 is not caused by skew scattering and only has a weak dependence on the relaxation period τ. It is clear that A0 0's Fermi-surface part contributes less to C than A0, notwithstanding a slow convergence with the transverse supercell size Ly. Furthermore, at ambient temperature, the

DOI : https://doi.org/10.5281/zenodo.22326694

International Journal of Sustainable Intelligent Technologies
ISSN: 3139-1249
IJSIT-05

Fermi-surface and Fermi-sea contributions to A0 0 cancel out, making them almost insignificant. The value of A0 is consistent with prior phenomenological broadening estimates and experimental measurements [58] for a Co/Pt bilayer with similar layer thicknesses.

Table I shows the coefficients (ns/m) for the angular expansion of the Co/Pt bilayer spin-orbit torque. The lateral supercell size, Ly, represented in a/− 2 units, only applies to the Fermi surface region. The energy E corresponds to EF ± 0.046 eV.

	E	L_y	Fermi surface, V_m (eV)				Fermi sea, T (K)			
			0.77	1.09	1.33	1.54	300	200	100	50
A_0	E_F	1	29.4	24.8	23.4	21.9	1.4	0.8	0.8	-1.3
	E_F	2	29.9	31.3	24.4	27.7				
	E_F	3		27.5						
	E_+	2		30.5						
	E_-	2		26.8						
A_0'	E_F	1	-5.2	-3.1	-2.6	-0.7	5.3	7.6	10.6	13.6
	E_F	2	-3.3	-10.7	-2.8	-7.5				
	E_F	3		-6.0						
	E_+	2		-4.7						
	E_-	2		-2.2						
A_2	E_F	2	-1.3	-2.2	-0.3	-0.9	0.6	1.4	3.2	6.3
$A_{\beta 0}$	E_F	2	-1.5	-0.3	0.0	0.0	0.3	1.4	5.2	7.3
B_0	E_F	1	-8.1	-8.0	-6.3	-4.1				
	E_F	2	-8.8	-5.0	-3.8	-1.7				
	E_F	3		-6.3			0			
	E_+	2		-7.5						
	E_-	2		-3.2						
B_0'	E_F	1	-6.8	-8.2	-10.7	-9.9				
	E_F	2	-7.5	-7.6	-6.8	-5.8				
	E_F	3		-8.3			0			
	E_+	2		-9.3						
	E_-	2		-8.3						

The odd torquance, as shown in Table I, has a significant B0 0 term of comparable magnitude to the basic field-like B0 term; all other terms are trivial. In contrast, computations using phenomenological broadening yielded no terms above B0. Consistent with the inverse spin-galvanic effect, the B0 coefficient drops as the strength of the diseq oscillation grows.

The odd torquance terms B0 0 and B2 contribute to damping, as shown by C = 3(B0 0+B2)mxmz, or the "planar Hall-like" damping observed when m is in the xz plane. Table I, like A0, indicates that the term B0 0 is insensitive to the degree of disorder. In all cases, the B2 word was determined to be insignificant.

The finding of significant words in the odd SOT beyond B0 is consistent with the experimental results. Although research on SOT in AlOx/Co/Pt and AlOx/Co/Pd reveals an approximation of the relationship B2 = - 2 3B0 0, our examination discovered high values of B0 0 and B2 ≈ 0 in a Co/Pt bilayer. Although the sign of B0 0 is different, the FMR linewidth measurements correlate to the relative magnitude of the damping parameter C measured in the xy (spin-Hall-like SOT) and xz (planar Hall-like SOT) planes.

Table I includes the Fermi-surface SOT coefficients calculated at energies E± = E ±0.046 eV.

DOI : https://doi.org/10.5281/zenodo.22326694

International Journal of Sustainable Intelligent Technologies
ISSN: 3139-1249
IJSIT-05

The value of (−∂ ·f /∂E) at these energies is 50% lower than its highest value at 300 K. The coefficients A0 and B0 0 show a mild energy dependency and a linear approximation, respectively, indicating that the Fermi temperature has no substantial effect on them. Notably, the A0 0 coefficient remains rather low.

Figure 4 shows atom-resolved contributions to the A0, A0 0, B0, and B0 0 terms at Vm = 1.09 eV; these quantities are also shown for comparison with the free-standing 6-monolayer Co film with the same lattice parameter, where the total torquance is eliminated due to symmetry.

Figure 4 shows atomic-resolved torquances at a vacuum potential (Vm) of 1.09 eV measured with Ly = 3 in the Co(6)Pt(6) bilayer (solid lines) and the free-standing Co(6) film (dashed lines). phrases A0 and A0 are even, but phrases B0 and B0 are odd. The light-blue curves (labeled ΄YPt = 0): A0 in the Co(6)Pt(6) obtained with Ly = 1. The SOC on Pt atoms is configured to zero.

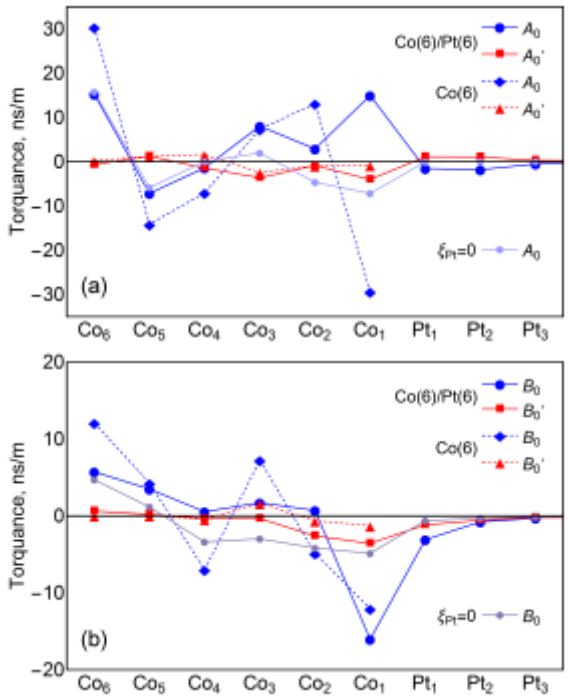

FIG. 4. Atom-resolved torquances in the Co(6)Pt(6) bilayer (solid lines) and in the free-standing Co(6) film (dashed lines) at Vm = 1.09 eV, obtained with Ly = 3. (a) Even terms A0 and A 0 0, (b) odd terms B0 and B 0 0. Light-blue curves (labeled ξPt = 0): A0 in Co(6)Pt(6) with SOC on Pt atoms set to zero, obtained with Ly = 1.

The contributions to A0 and B0 are proportional to the thickness of the film. The Co atoms nearest to the Co/Pt interface and those on the free surface of Co contribute the most. In contrast, the B0 0 word appears to originate at the Co/Pt interface. Pt atoms near the interface contribute significantly to B0, with a magnetic moment of 0.24μB due to the proximity effect. In fact, the SOT of Pt atoms accounts for up to

Finally, we examine the SOT using a supercell with Ly = 2 and the SOC on Pt atoms switched off. In essence, the A0 term vanishes, albeit as shown in Figure. Atom-resolved contributions remain large in 4(a), and those near the free Co surface rarely change. The B0 0

DOI : https://doi.org/10.5281/zenodo.22326694

term, like the averaging error, is significantly suppressed from −7.6 to −1.4 ns/m. The B0 term has a significant redistribution of atom-resolved contributions, increasing to −10.8 ns/m [Fig.]. 4. These results suggest that the SOT in our Co/Pt bilayer is almost non-dissipative, or that it has no influence on magnetization damping in the absence of SOC on Pt. Formally, the Dzyaloshinskii-Moriya interaction caused by current generates atom-resolved torques that resemble damping and sum to zero. Thus, a heavy-metal layer is not required for strong field-like SOT; nonetheless, more research is needed to understand the circumstances that must be met in order to observe damping-like SOT in the absence of heavy metals.

Finally, we showed that the SOT of a Co/Pt bilayer can be computed using the density-functional-theory NEGF formalism and an explicit disorder model. We found terms that go beyond the typical damping- and field-like torques, such as a large planar Hall-like B0 0 term [Eq. This observation is consistent with the FMR measurements. The dissipative portion of the SOT is almost entirely due to the SOC on Pt atoms.

We sincerely thank YaroslavTserkovnyak, Igor Zuti'c, Farzad Mahfouzi, Branislav Nikoli'c, Ilya Krivorotov, and Vladimir Antropov for their insightful conversations. The National Science Foundation (NSF) provided financial support for UNL's research under Grant No. The Nebraska Military Research, Science, and Engineering Center (MR SEC, Grant Numbers DMR-DMR-1420645 and DMR-1609776). A.K. received aid from the United States of America. The Department of Energy's grant No. de sc0014189 aided the work even further.

REFERENCES

1. A. Manchon, I. M. Miron, T. Jungwirth, J. Sinova, J. Zelezn´y, A. Thiaville, K. Garello, and P. Gambardella, ArXiv e-prints (2018), arXiv:1801.09636.
2. R. Ramaswamy, J. M. Lee, K. Cai, and H. Yang, Appl. Phys. Rev. 5, 031107 (2018).
3. K. Garello, C. O. Avci, I. M. Miron, M. Baumgartner, A. Ghosh, S. Auffret, O. Boulle, G. Gaudin, and P. Gambardella, Appl. Phys. Lett. 105, 212402 (2014).
4. S.-H. Yang, K.-S. Ryu, and S. Parkin, Nat. Nanotechnol. 10, 221 (2015).
5. S. V. Aradhya, G. E. Rowlands, J. Oh, D. C. Ralph, and R. A. Buhrman, Nano Lett. 16, 5987 (2016).
6. G. Prenat, K. Jabeur, P. Vanhauwaert, G. D. Pendina, F. Oboril, R. Bishnoi, M. Ebrahimi, N. Lamard, O. Boulle, K. Garello, J. Langer, B. Ocker, M. Cyrille, P. Gambardella, M. Tahoori, and G. Gaudin, IEEE Trans. Multi-Scale Computing Syst. 2, 49 (2016).
7. S. Fukami and H. Ohno, Jpn. J. Appl. Phys. 56, 0802A1 (2017).
8. L. Liu, C.-F. Pai, D. C. Ralph, and R. A. Buhrman, Phys. Rev. Lett. 109, 186602 (2012).
9. V. E. Demidov, S. Urazhdin, H. Ulrichs, V. Tiberkevich, A. Slavin, D. Baither, G. Schmitz, and S. O. Demokritov, Nat. Mater. 11, 1028 (2012).
10. Z. Duan, A. Smith, L. Yang, B. Youngblood, J. Lindner, V. E. Demidov, S. O. Demokritov, and I. N. Krivorotov, Nat. Commun. 5, 5616 (2014).

DOI : https://doi.org/10.5281/zenodo.22326694